AFRL-ML-WP-TP-2006-467

PREDICTION OF CRYSTALLOGRAPHIC TEXTURE EVOLUTION AND ANISOTROPIC STRESS-STRAIN CURVES DURING LARGE PLASTIC STRAINS IN HIGH PURITY α-TITANIUM USING A TAYLOR-TYPE CRYSTAL PLASTICITY MODEL (PREPRINT)

Xianping Wu, Surya R. Kalidindi, Carl Necker, and Ayman Salem

SEPTEMBER 2006

Approved for public release; distribution is unlimited.

STINFO COPY

MATERIALS AND MANUFACTURING DIRECTORATE
AIR FORCE RESEARCH LABORATORY
AIR FORCE MATERIEL COMMAND
WRIGHT-PATTERSON AIR FORCE BASE, OH 45433-7750

REPORT DOCUMENTATION PAGE

Form Approved
OMB No. 0704-0188

1. REPORT DATE *(DD-MM-YY)*	2. REPORT TYPE	3. DATES COVERED *(From - To)*
September 2006	Journal Article Preprint	N/A

4. TITLE AND SUBTITLE

PREDICTION OF CRYSTALLOGRAPHIC TEXTURE EVOLUTION AND ANISOTROPIC STRESS-STRAIN CURVES DURING LARGE PLASTIC STRAINS IN HIGH PURITY α-TITANIUM USING A TAYLOR-TYPE CRYSTAL PLASTICITY MODEL (PREPRINT)

5a. CONTRACT NUMBER
F33615-03-D-5801

5b. GRANT NUMBER

5c. PROGRAM ELEMENT NUMBER
62102F

6. AUTHOR(S)

Xianping Wu and Surya R. Kalidindi (Drexel University)
Carl Necker (Los Alamos National Laboratory)
Ayman Salem (AFRL/MLLM and Universal Technology Corporation)

5d. PROJECT NUMBER
4349

5e. TASK NUMBER
L0

5f. WORK UNIT NUMBER
VT

7. PERFORMING ORGANIZATION NAME(S) AND ADDRESS(ES)

Drexel University
Department of Materials Science and Engineering
Philadelphia, PA 19104

Los Alamos National Laboratory
Materials Science and Technology Division
Los Alamos, NM 87545

Metals Branch (AFRL/MLLM)
Metals, Ceramics, and Nondestructive Evaluation Division
Materials and Manufacturing Directorate
Air Force Research Laboratory, Air Force Materiel Command
Wright-Patterson Air Force Base, OH 45433-7750

Universal Technology Corporation
Dayton, OH 45432

8. PERFORMING ORGANIZATION REPORT NUMBER

9. SPONSORING/MONITORING AGENCY NAME(S) AND ADDRESS(ES)

Materials and Manufacturing Directorate
Air Force Research Laboratory
Air Force Materiel Command
Wright-Patterson AFB, OH 45433-7750

10. SPONSORING/MONITORING AGENCY ACRONYM(S)
AFRL-ML-WP

11. SPONSORING/MONITORING AGENCY REPORT NUMBER(S)
AFRL-ML-WP-TP-2006-467

12. DISTRIBUTION/AVAILABILITY STATEMENT

Approved for public release; distribution is unlimited.

13. SUPPLEMENTARY NOTES

Journal article submitted to Acta Materialia, published by Elsevier B.V.

Paper contains color. PAO Case Number: AFRL/WS 06-1768, 14 Jul 2006.

14. ABSTRACT

A new Taylor-type polycrystalline model has been developed to simulate the evolution of crystallographic texture and the anisotropic stress-strain response during large deformation of high purity α-titanium at room temperature. Crystallographic slip, deformation twinning, and slip inside the twinned regions were all considered as contributing mechanisms for the plastic strain in the model. This was accomplished by treating the dominant twin systems in a given crystal as independent grains once the total twin volume fraction in that crystal reached a predetermined saturation value. The newly formed grains were allowed to independently undergo further slip and the concomitant lattice rotation, but further twinning was prohibited. New descriptions have been proposed for slip and twin hardening and the complex coupling between them. Good predictions were obtained for the overall anisotropic stress-strain response and the texture evolution in three different monotonic deformation paths on annealed, initially textured samples of high purity α-titanium.

15. SUBJECT TERMS Twinning, Plastic, Hardening, Texture, Anisotropic

16. SECURITY CLASSIFICATION OF:			17. LIMITATION OF ABSTRACT:	18. NUMBER OF PAGES	19a. NAME OF RESPONSIBLE PERSON (Monitor)
a. REPORT	b. ABSTRACT	c. THIS PAGE			S.L. Semiatin
Unclassified	Unclassified	Unclassified	SAR	32	19b. TELEPHONE NUMBER *(Include Area Code)* N/A

Prediction of crystallographic texture evolution and anisotropic stress-strain curves during large plastic strains in high purity α-Titanium using a Taylor-type crystal plasticity model

Xianping Wu[1], Surya R. Kalidindi[1], Carl Necker[2] and Ayman Salem[3,4]

[1]Department of Materials Science and Engineering, Drexel University, Philadelphia, PA 19104
[2]Materials Science and Technology Division, Los Alamos National Laboratory, NM 87545
[3]Air Force Research Laboratory, AFRL/MLLM, Wright-Patterson AFB, OH 45433
[4] Universal Technology Corporation, Dayton, OH 45432

Abstract - A new Taylor-type polycrystalline model has been developed to simulate the evolution of crystallographic texture and the anisotropic stress-strain response during large deformation of high purity α-titanium at room temperature. Crystallographic slip, deformation twinning, and slip inside the twinned regions were all considered as contributing mechanisms for the plastic strain in the model. This was accomplished by treating the dominant twin systems in a given crystal as independent grains once the total twin volume fraction in that crystal reached a predetermined saturation value. The newly formed grains were allowed to independently undergo further slip and the concomitant lattice rotation, but further twinning was prohibited. New descriptions have been proposed for slip and twin hardening and the complex coupling between them. Good predictions were obtained for the overall anisotropic stress-strain response and the texture evolution in three different monotonic deformation paths on annealed, initially textured samples of high purity α-titanium.

*Keywords***:** Twinning; Plastic; Hardening; Texture; Anisotropic

1. Introduction

A rigorous formulation of the elastic-plastic constitutive relations for crystalline materials undergoing finite plastic strains by crystallographic slip alone is now well established in literature [1-8]. However, many materials exhibit deformation twinning as an additional mode of plastic deformation, especially at low homologous temperatures and/or high strain rates [9-11]. Several studies have reported extensive deformation twinning in room (and lower) temperature deformation of α-Ti [12-19]. Consequently, it is highly desirable to extend the current crystal plasticity theories to include deformation twinning as an additional mode of plastic deformation. The main obstacle in accomplishing this goal is the lack of an efficient method to handle the extremely large number of new orientations created by deformation twinning. Three different approaches have been proposed in the literature to address this problem:

(1.) Predominant Twin Reorientation (PTR) Method: This method was originally proposed by Van Houtte [20] and improvements were made by Tome et al. [21]. Staroselsky and Anand [22, 23] have formulated a rigorous and efficient numerical approach for the use of rate-independent crystal plasticity theories and applied it with the PTR model to study stress-strain responses and texture evolution in low stacking fault energy cubic and hexagonal metals. Kaschner et al. [24] employed the PTR method in a visco-plastic self-consistent crystal plasticity modeling framework to study the role of twinning in the hardening response of zirconium during temperature reloads. In the PTR scheme, twinning is essentially treated as a pseudo-slip mechanism while the evolution of the volume fractions of the twinned regions is carefully tracked in each grain. Consequently, the twinned regions are not reoriented at the end of each time step. Instead, a statistical criterion is devised and employed to ensure that an appropriate number of heavily twinned grains are completely reoriented into their predominant twin

orientations; this number is selected based on the total volume fraction of twinned regions in the entire polycrystal. A major advantage of this method is that the number of total grain orientations remains constant during the entire simulation. The disadvantage of this method is that it can not be applied at the single crystal level and is not particularly amenable to the highly efficient, total Lagrangian, fully implicit time integration procedure developed recently for the crystal plasticity constitutive framework [2].

(2.) Volume Fraction Transfer (VFT) Scheme: This approach was proposed by Tome et al. [21] and employs weighted (and binned) grain orientations to address the problem of tracking the large number of new orientations created by deformation twinning. In this scheme, the relevant Euler space of distinct grain orientations (also called the fundamental zone of orientations [25]) is suitably binned and the texture in the sample is represented by the weights associated with the binned orientations. Therefore, only the weights of the grain orientations need to be suitably modified to reflect the orientation changes caused by twinning, and hence there is no need to create new orientations. However, the disadvantages of this method are that a very large number of bins are needed (especially for the lower symmetry hexagonal metals) and that this approach is also not particularly amenable for implementation of the efficient fully implicit time integration procedure developed recently for the crystal plasticity constitutive framework.

(3.) Total Lagrangian Approach: Building on a total Lagrangian crystal plasticity framework that was initially formulated for materials that exhibit only crystallographic slip [2], Kalidindi [26] proposed a new interpretation of the multiplicative decomposition of the total deformation gradient into its elastic and plastic components when deformation twinning is added as an additional mode of plastic deformation. The main advantages of this method are that it allows the application of the crystal plasticity theory with deformation twinning to a single crystal while

taking full advantage of the efficient fully implicit time integration schemes that have been previously developed and validated. The disadvantage of this method continues to be the fact that the numerical implementation of the scheme is quite cumbersome when slip inside the twinned regions is to be allowed as a significant contribution to the plastic deformation in the crystal. The importance of including slip inside twins as an additional mode of plastic deformation was established in a recent experimental study [12, 17, 19], where it was observed that the averaged Taylor factor for the twinned regions in a sample of high purity α-Ti deformed in simple compression was about 40% lower than that for the matrix regions, implying that the slip inside the twinned regions would be a significant component of the overall plastic deformation in this sample. In our prior modeling effort in low stacking fault energy fcc metals, the fact that the potential twin systems are co-planar with the potential slip systems made it relatively easy to incorporate slip inside twinning as a contribution to the overall plastic deformation [27]. However, the potential twin systems in hcp metals are non-coplanar with all of the potential slip systems, and therefore tracking the slip activity inside the already formed twins becomes quite cumbersome in this approach.

It is therefore clear that there exist a number of outstanding problems in the incorporation of deformation twinning in the current crystal plasticity modeling framework. Recent experimental studies [12, 19] have provided several new insights that, in turn, suggest new simplifying approximations to overcome some of the difficulties described above in the modeling efforts. Of particular importance to the work presented here is the observation reported by Salem et al. [19] that much of the deformation twinning in high purity α-Ti deformed in simple compression at room temperature occurred in a relatively narrow moderate strain range of 0.05 to 0.3 (with most of the profuse twinning actually occurring in an even narrower strain range of 0.15-0.20). At

higher strain levels, the grain structure fragmented substantially and the rate of deformation twinning decreased dramatically. Although the precise reason for the shutdown of deformation twin production at high strains is not yet fully understood, it is generally attributed to the much higher stresses required to produce the shorter deformation twins in the smaller fragmented grains [28].

The main objective of the present paper is to report on our latest effort to develop an improved Taylor-type crystal plasticity model for α-Ti hcp polycrystals. This new model employs a grain fragmentation concept. In this new model, following the earlier approaches [20, 29], deformation twinning is initially treated as a pseudo-slip mechanism. When a certain volume fraction of any grain has undergone deformation twinning, that particular grain is fragmented into its dominant twin systems. In subsequent deformation, neither the parent grain nor any of its newly formed fragmented components are allowed to produce deformation twins. The main motivation for exploring this approach stems from the previously described observations in α-Ti where it was noted that deformation twinning dominates the texture evolution in the polycrystal in a short intermediate strain regime [19, 28]. Therefore, the underlying approximations in the proposed approach should have very little effect on the texture evolution of the polycrystal at large strains. Furthermore, since the grain is allowed to fragment only once and only into its dominant twin components, the number of new grains produced is relatively small and can be efficiently handled with only a moderate increase in the computational effort. Finally, the proposed approach can be easily implemented in the previously established, numerically efficient, total Lagrangian framework with the associated fully implicit time integration procedure [2]. In many ways, the proposed approach here combines the best aspects of the different modeling approaches described earlier [20, 21, 26]. Furthermore, the slip-

twin hardening functions have been expanded from the previously used versions [29], and have been observed to provide better predictions of the anisotropic stress-strain responses in a range of deformation experiments.

2. A New Crystal Plasticity Model for High Purity α-Ti

A new Taylor-type crystal plasticity model is presented here for room temperature deformation of high purity α-Ti using a notation that is now standard in this field [30]. In this notation, **F** represents the deformation gradient tensor, **L** represents the velocity gradient tensor, and **T** represents the Cauchy stress tensor. An important feature of the model presented here is the introduction of a grain[1] fragmentation event based on the accumulated deformation twinning activity in the crystal. The details of the grain fragmentation event and the behavior of the grain prior and subsequent to this fragmentation event are described next.

2.1 Grains Prior to Fragmentation

The grains prior to fragmentation are modeled using essentially the approach described previously by Kalidindi [26], with some modifications in the strain hardening descriptions. The imposed total deformation gradient tensor on the crystal is multiplicatively decomposed into two components (see Figure 1):

$$\mathbf{F} = \mathbf{F}^{*}\mathbf{F}^{p} . \tag{1}$$

[1] The individual crystals comprising a polycrystal are commonly referred to as grains in metallurgy.

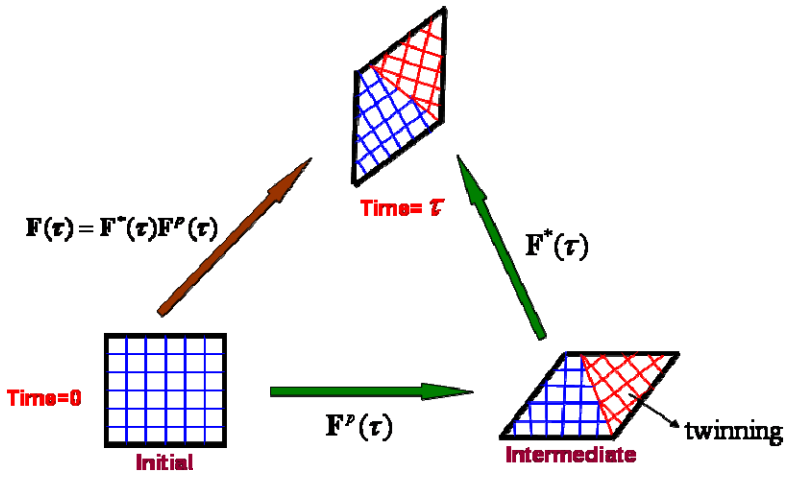

Figure 1. A schematic of the interpretation of the multiplicative decomposition of deformation gradient when twinning is included [26].

In this model, $\mathbf{F}^p$ denotes the plastic deformation gradient tensor that describes the overall (effective) shape change induced in the grain as a consequence of the crystallographic slip and deformation twinning in the grain, while $\mathbf{F}^*$ denotes the additional transformation (including elastic stretch and rotations) needed to account for the total imposed shape change induced by **F.** It is further assumed that the slip processes leave the lattice orientation unchanged, while deformation twinning rotates the lattice into a priori defined orientation (for the hexagonal crystals of interest in this paper this relationship is conveniently described as a 180 degree rotation about the twin plane normal [9]). Consequently, the orientations of the twinned and untwined regions of the grain in the hypothetical intermediate configuration shown in Figure 1 (after the application of $\mathbf{F}^p$) are fully known a priori, given the initial orientation of the grain. As a consequence of the above definition of $\mathbf{F}^p$, the polar decomposition of $\mathbf{F}^\bullet$ provides the elastic stretch and the overall lattice rotation between the intermediate configuration and the deformed configuration. In Figure 1, only one twin system is shown for clarity. However, multiple twin systems are allowed in one grain. Furthermore, the twinned region belonging to one twin system

is idealized as a continuous block, while in reality, deformation twins occur as thin plates. This simplification was motivated by the reported experimental observations in literature [12, 17, 31], which suggest that the deformation twins of a particular twin system occur as clusters of roughly parallel plates of similar lattice orientation in any given grain. The fact that the twins occur as clusters of parallel plates does have a major influence on the hardening response of the crystal, and this aspect will be treated later using appropriate phenomenological slip and twin hardening laws.

The constitutive equation for the elastic response of a single crystal is expressed as

$$\mathbf{T}^{*} = \mathbf{C}\left[\mathbf{E}^{*}\right], \tag{2}$$

where $\mathbf{C}$ represents the fourth-order anisotropic elasticity tensor, $\mathbf{T}^{*}$ and $\mathbf{E}^{*}$ are a pair of work conjugate stress and strain measures defined as

$$\mathbf{T}^{*} = \mathbf{F}^{*-1}\{(\det\mathbf{F}^{*})\mathbf{T}\}\mathbf{F}^{*-T} \quad , \tag{3}$$

$$\mathbf{E}^{*} = \frac{1}{2}\{\mathbf{F}^{*T}\mathbf{F}^{*} - 1\} . \tag{4}$$

The evolution of plastic deformation gradient can be expressed as

$$\dot{\mathbf{F}}^{\mathrm{p}} = \mathbf{L}^{\mathrm{p}}\mathbf{F}^{\mathrm{p}} , \tag{5}$$

where $\mathbf{L}^{\mathrm{p}}$ is plastic velocity gradient tensor expressed as

$$\mathbf{L}^{\mathrm{p}} = \sum_{\alpha}^{N^{s}} \dot{\gamma}^{\alpha}\mathbf{S}_{o}^{\alpha} + \sum_{\beta}^{N^{tw}} \dot{f}^{\beta}\gamma_{tw}^{\beta}\mathbf{S}_{o}^{\beta} . \tag{6}$$

The two terms on the right hand side of Eq. (6) represent the contributions to plastic deformation by slip and deformation twinning respectively. $\mathbf{S}$ denotes the unit slip (twin) tensor, defined as the dyadic product of two orthogonal unit vectors denoting the slip (twin shear) direction and the slip (twin) plane normal, respectively. The subscript o on $\mathbf{S}$ reminds us that these are defined

using the initial crystal orientation and therefore the **S** tensors are known a priori. The superscripts α and β enumerate the available slip systems (total of N^s) and the available twin systems (total of N^{tw}), respectively. $\dot{\gamma}^\alpha$ represents the slip shear rate on slip system α. Unlike slip, deformation twinning is characterized by a constant amount of shear and the volume fraction of the crystal experiencing deformation twinning evolves with the imposed deformation. Treating deformation twinning as a pseudo-slip mechanism, the homogenized shear rate in the crystal is described by $\dot{f}^\beta \gamma_{tw}^\beta$, where γ_{tw}^β represents the amount of constant shear associated with twin system β and f^β denotes its volume fraction in the given crystal.

Power-law relations have been employed to quantify the plastic shearing rate on slip and twin systems using the visco-plastic approach of Asaro and Needleman [4]:

$$\dot{\gamma}^\alpha = \dot{\gamma}_o \left| \frac{\tau^\alpha}{s^\alpha} \right|^{1/m} sign(\tau^\alpha), \tag{7}$$

$$\dot{f}^\beta = \begin{cases} \dfrac{\dot{\gamma}_o}{\gamma_{tw}^\beta} \left| \dfrac{\tau^\beta}{s^\beta} \right|^{1/m} & \text{if} \quad \tau^\beta \geq 0 \\ 0 & \text{if} \quad \tau^\beta \leq 0 \end{cases}. \tag{8}$$

In this study, the rate sensitivity parameter, *m*, was assumed to be the same for both slip and twinning. A very low value of $m = 0.02$ was used to simulate almost rate-independent behavior of metals at room temperature. The reference slip rate, $\dot{\gamma}_o$, was arbitrarily set as 0.001 s^{-1} to reflect our interest in quasi-static loading conditions. τ^α and s^α represent the resolved shear stress and the shear resistance for a particular slip or twin system. Note that, unlike slip, a positive resolved shear stress is needed for twinning. The resolved shear stress for both slip and twin systems can be defined as [2]

$$\tau^{\alpha} \approx \mathbf{T}^{*} \bullet \mathbf{S}_{o}^{\alpha} . \tag{9}$$

Description of the evolution of the slip and twin resistances during plastic deformation has been a very difficult problem in the development of robust crystal plasticity models for hcp metals such as Ti. The slip-twin interactions are fairly complex [12, 17, 19, 32, 33], and there is thus far only a limited amount of quantitative experimental data available. In this study, following the current efforts in literature, we employed a phenomenological description of the slip and twin hardening laws. Some of the most successful phenomenological descriptions to date have been the saturation-type hardening laws that can be generically expressed as

$$\dot{s}^{\alpha} = h_{s}^{\alpha}(1-\frac{s^{\alpha}}{s_{s}^{\alpha}})\sum_{k}^{N^{s}}\dot{\gamma}^{k} , \tag{10}$$

where h_s^{α} and s_s^{α} represent the hardening rate and the saturation value associated with the slip system α, respectively. Implicit in Eq. (10) is the assumption of isotropic latent hardening which implies that activity on one slip system results in equal hardening of all potential slip systems. In a recent paper, Salem et al. [29] used extended versions of the saturation-type hardening functions to capture the complex interactions between slip and twinning. In that study, Eq. (10) has been used for slip hardening, while allowing the slip hardening rate and the saturation values to evolve with deformation twin activity as

$$h_{s}^{\alpha} = h_{s}(1 + C(\sum_{\beta} f^{\beta})^{b}) , \tag{11}$$

$$s_{s}^{\alpha} = s_{so} + s_{pr}(\sum_{\beta} f^{\beta})^{0.5} . \tag{12}$$

The functional forms of Eqs. (11) and (12) were motivated by experimental observations in deformation studies on high-purity α-Ti [12, 17, 19, 28]. The parameters h_s and s_{so} denote the

hardening rate and the saturation value, respectively, in the absence of twinning. C, s_{pr} and b are hardening parameters that aim to capture phenomenologically the complex interactions between slip and deformation twinning. $\sum_{\beta} f^{\beta}$ denotes the total twin volume fraction in the grain.

In the present work, we found it essential to allow the hardening parameters in Eqs. (11) and (12) to take on different values for the different slip families in order to obtain better predictions of the anisotropic stress-strain responses in α-Ti subjected to different deformation paths. Table 1 provides a summary of the different slip and twin families considered in this study. A total of 18 slip systems belonging to three distinct slip families and 12 twin systems belonging to two distinct twin families were considered. Consequently, Eqs. (10) - (12) were reformulated for the present study as

$$\dot{s}^{\alpha} = h_s^{pri}(1-\frac{s^{\alpha}}{s_s^{\alpha}})\sum_{k}^{N_{pri}^{s}}\dot{\gamma}^{k} + h_s^{bas}(1-\frac{s^{\alpha}}{s_s^{\alpha}})\sum_{l}^{N_{bas}^{s}}\dot{\gamma}^{l} + h_s^{pyr}(1-\frac{s^{\alpha}}{s_s^{\alpha}})\sum_{m}^{N_{pyr}^{s}}\dot{\gamma}^{m}\ , \tag{13}$$

$$h_s^{pri} = h_{so}^{pri}(1+C(\sum_{\beta} f^{\beta})^{b})\ ,\ h_s^{bas} = h_{so}^{bas}(1+C(\sum_{\beta} f^{\beta})^{b})\ , h_s^{pyr} = h_{so}^{pyr}(1+C(\sum_{\beta} f^{\beta})^{b})\ , \tag{14}$$

$$s_s^{\alpha} = \begin{cases} s_{so}^{pri} + s_{pr}(\sum_{\beta} f_{\beta})^{0.5} & if \quad \alpha \in \text{prism slip systems} \\ s_{so}^{bas} + s_{pr}(\sum_{\beta} f_{\beta})^{0.5} & if \quad \alpha \in \text{basal slip systems} \\ s_{so}^{pyr} + s_{pr}(\sum_{\beta} f_{\beta})^{0.5} & if \quad \alpha \in \text{pyramidal slip systems} \end{cases} . \tag{15}$$

Table1. Summary of Slip and Twin systems

	Slip Systems			Twin Systems	
Family	Prismatic <a>	Basal <a>	Pyramidal<c+a>	Compressive	Tensile
Plane & Direction	$\{10\bar{1}0\}<11\bar{2}0>$	$\{0001\}<11\bar{2}0>$	$\{10\bar{1}1\}<11\bar{2}3>$	$\{11\bar{2}2\}<11\bar{2}\bar{3}>$	$\{10\bar{1}2\}<\bar{1}011>$

Number of systems	3	3	12	6	6
Initial resistance	s_o^{pri}	s_o^{bas}	s_o^{pyr}	s_{tw}^{com}	s_{tw}^{ten}
Slip family specific hardening parameters	$h_{so}^{pri}, s_{so}^{pri}$	$h_{so}^{bas}, s_{so}^{bas}$	$h_{so}^{pyr}, s_{so}^{pyr}$	*No hardening parameters needed for twin systems.*	
Common hardening parameters	C, b, s_{spr}				

The experimental observations of Salem et al. [12, 17] indicate that twinning occurs profusely in a short intermediate strain range. Consequently, we have decided to treat the twin resistances as constants prior to grain fragmentation.

2.2 Criterion for Grain Fragmentation

In the present model, when the twin volume fraction in a given grain ($\sum_{\beta} f^{\beta}$) reaches a predetermined saturation value (f_{sat}), that grain is fragmented into parts: a parent grain (corresponding to the untwinned or matrix region) and several offspring grains (corresponding to the dominant twinning activity in that grain). In this study, f_{sat} was set equal to 0.4 based on the experimental observations reported by Salem et al. [12, 19]. The volume fractions of the parent and the offspring grains are determined by the accumulated twinning activity in the grain up to the point of fragmentation. It is ensured that the sum of the volume fractions of the parent and the offspring grains is equal to one. Once the grain is fragmented, the volume fractions of the newly created grains are kept constant during the rest of the deformation. Consequently, the number of new orientations produced in this model simply equals to the number of offspring grains created in the fragmentation process. In this study, only the twin systems with a volume fraction of over 0.1 were represented in the newly created grains. The volume fractions

associated with the non-dominant twin systems (defined here as $f^{\beta} < 0.1$) have been transferred to the most dominant twin system.

2.3 Grains after Fragmentation

In this study, the slip resistances of the various slip systems in the parent and offspring grains have been assigned the same values that were in the grain prior to fragmentation. However, the resistance for any twin system in the parent and the offspring grains is assumed to be very high so that no further twinning can be activated. The evolution of slip resistances in subsequent deformation continues as described by Eqs. (13) – (15). Note that the slip activities in the offspring grains are tantamount to slip in the twinned regions of the original grain. After grain fragmentation, the newly formed grains (parent and offspring grains) are essentially treated as independent grains. Moreover, further plastic deformation in these grains is assumed to be fully accommodated by crystallographic slip alone. Note that, in the total Lagrangian framework employed in this work, the slip tensors ($\mathbf{S}_o^{\alpha}$ in Eq. (6)) in the newly created grains are defined based on the orientations of the twinned regions in the intermediate relaxed configuration. As noted earlier, the twin orientations in the intermediate configuration are known a priori, and are conveniently described by a 180 degree rotation about the twin habit plane for the α-Ti single crystals studied here.

The treatment of the grains before and after fragmentation is summarized in Figure 2. The following salient features of the new model presented here are worth noting:

(1.) Before fragmentation, deformation twinning is treated as a pseudo-slip mechanism. So there is only a single decomposition of the total deformation gradient tensor. Consequently, the matrix and the twinned regions have a pre-defined orientation relationship. In other words,

the twin regions rotate with the matrix as if they were rigid inclusions attached to the matrix with a specific orientation relationship.

(2.) After fragmentation, the newly formed grains behave independent of the parent grain and each other. Following the Taylor approach [34], the matrix and twin are assumed to experience the same total deformation gradient tensor. However, the plastic deformation gradient, the elastic deformation gradient, and the lattice rotation are expected to differ substantially among the parent and each of the offspring grains. Note also that the special orientation relationship between the parent and offspring grains is still maintained in the intermediate relaxed configuration (even after grain fragmentation), but is expected not to be retained in the final configuration (because the parent and offspring grains are generally expected to experience different lattice rotations after the fragmentation event).

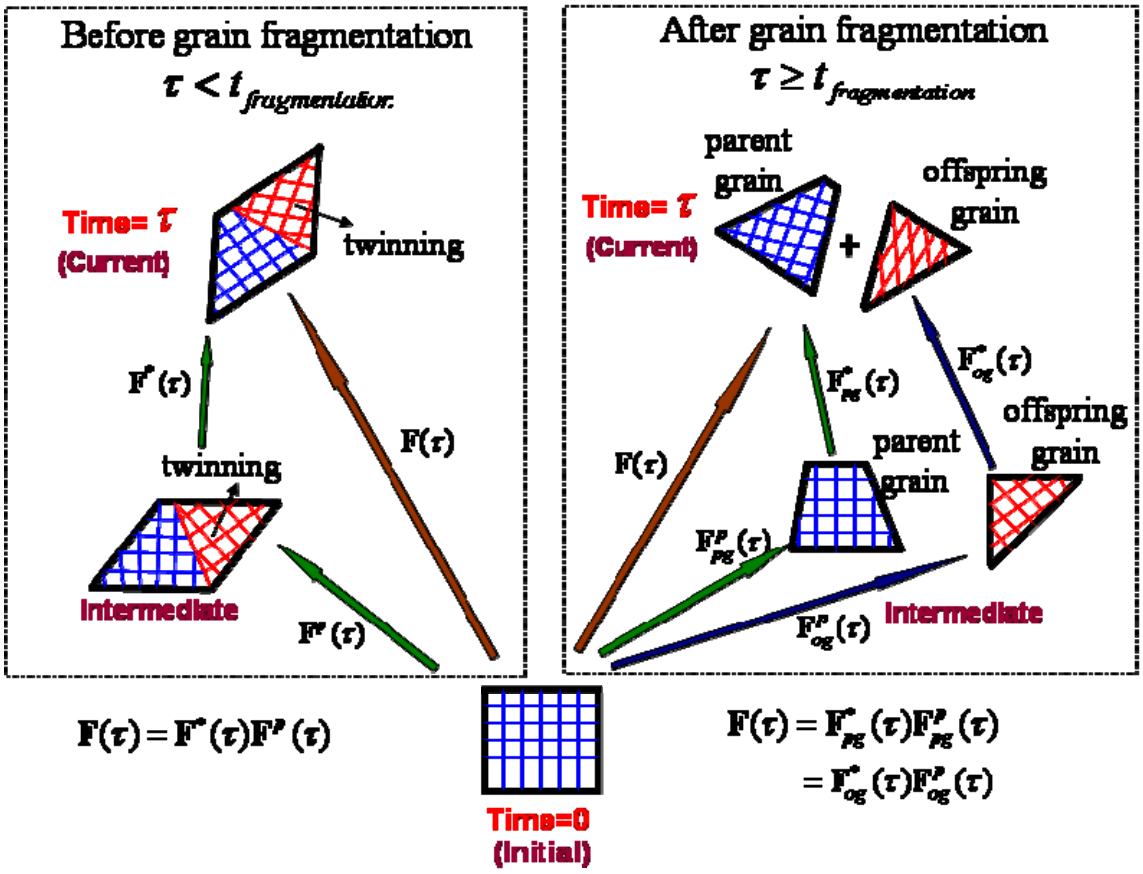

Figure 2. Summary of the multiplicative decomposition of the total deformation gradient implemented in the model presented in this study. *pg* denotes the parent grain and *og* denotes the offspring grain. Only one offspring is shown in the figure for clarity.

The response of a polycrystalline aggregate is obtained here using the extended Taylor assumption of uniform deformation gradient tensor in the entire polycrystal [34]. Consequently, the overall Cauchy stress tensor in the polycrystal is assumed to be given by the volume averaged value of the Cauchy stress tensor in all of the constituent grains (including all of the parent and the offspring grains).

3. Experiments on High Purity α-Ti

The material used in this study was a high purity α-titanium (99.9998%) supplied by the Alta Group of Johnson Matthey Electronics, Inc., Spokane, WA. The received material was a circular plate with 352 mm diameter and 12 mm thickness. This material was recrystallized at 800°C for 1 hour and followed by water quench, producing an equiaxed grain structure with a 30 μm average grain size. The annealed sample showed a strong fiber texture (see Figure 5). The (0001) pole figures in figure 5 indicate that the c-axes of many grains in this sample lie about 20-35 degrees to the plate normal (labeled ND). Directions RD and TD were marked arbitrarily on the plane of the plate surface as shown in Figure 5. Additional information about this material can be obtained from the references [12, 17, 19].

Three stress-strain measurements (two from simple compression tests and one from simple shear test) on this material and the corresponding strain hardening plots were available from previous studies [12, 17, 29]. Measurements of the initial texture (Figure 5) and the measurement of deformed texture in simple shear test were also available from the earlier work [29]. Two new measurements of the deformed textures in simple compression tests were acquired for this study. These new measurements were obtained by X-ray reflection technique on a Scintag X1 5-axis pole figure goniometer using Cu-Kα radiation. The beam is point source, circularly collimated to 0.8mm. The

detector is a Peltier cooled solid state detector with a slit of 2mm. The samples were a minimum of 1 cm^2. The $(10\bar{1}0)$, (0001), $(10\bar{1}1)$, $(10\bar{1}2)$, $(11\bar{2}0)$ and $(10\bar{1}3)$ pole figures were measured. The samples were oscillated 4 mm to collect data from as many grains as possible. Data was collected out to 80 sample tilt in 5 sample rotation and tilt increments with a two second counting time. The data was analyzed using the popLA software [35], to produce corrected and recalculated pole figures and orientation distributions. The raw data was corrected for background and defocusing using a correction file generated from a titanium sample with a random texture. The data was then run through a harmonics algorithm to extrapolate the outer fringes of the pole figure data and then the data was re-normalized. This data was run through the WIMV algorithm to produce recalculated pole figures and orientation distributions.

4. Calibration and Evaluation of Model

4.1 Calibration: determination of model parameters

There are a total of fourteen material parameters in the crystal plasticity model presented in the previous section (see Table 1). Our goal is to establish the values of these parameters by curve-fitting the predicted stress-strain responses in selected deformation modes to the corresponding experimental measurements. In previous studies [29], we have established an approach for accomplishing this task. Our approach recognizes the influence the different parameters have on the form of the predicted stress-strain curves and uses repeated trials until the predictions match the measurements. In this process, in the present study, we noted that some of the parameters for the different slip families in Eqs. (13)-(15) exhibited values very close to each other. Based on these observations, we made the following assumptions for the present study that reduced the hardening parameters from fourteen to eleven:

$$h_{so}^{pri} = h_{so}^{bas} = h_{so}^{pri-bas}, \qquad s_{so}^{bas} = s_{so}^{pyr} = s_{so}^{bas-pyr}, \qquad s_{tw}^{com} = s_{tw}^{ten} = s_{tw} \tag{16}$$

The values of all the eleven parameters were established by fitting the predicted stress-strain curves to the corresponding measurements in two different monotonic deformation modes

(simple compression and simple shear). Briefly, our strategy for establishing the hardening parameters comprised of the following steps [29]:

(1) The values of initial resistances (s_o^{pri} , s_o^{bas} and s_o^{pyr}) on different slip families (basal <a>, prism <a> and pyramidal <c+a>) were determined by fitting the predicted yield strengths in simple compression along ND and in simple shear to the corresponding measurements (see Figure 3).

(2) The value of initial resistance (s_{tw}) for twinning was determined by matching the start of stage B in the predicted strain hardening plot in simple compression along ND (Point 2 in Figure 4) to the corresponding measurement. In a recent report [12], this point on the strain hardening plot curve has been correlated with the onset of deformation twinning.

(3) The values of slip hardening parameters ($h_{so}^{pri-bas}$, h_{so}^{pyr} , s_{so}^{pri} and $s_{so}^{bas-pyr}$) were determined by fitting the stage A of strain hardening plot (see Figure 4) and the stress-strain curve in simple shear (see Figure 3) where the volume fraction of deformation twinning is not significant and therefore slip is considered as the main mechanism to accommodate plastic deformation.

(4) The values of twin hardening parameters (b and C) were determined by fitting the stage B of strain hardening plot (see Figure 4) where the increment of strain hardening rate is correlated to the increasing twin volume fraction.

(5) The value of twin hardening parameter (s_{pr}) was determined by fitting the saturated flow stress in simple compression along ND (see Figure 3).

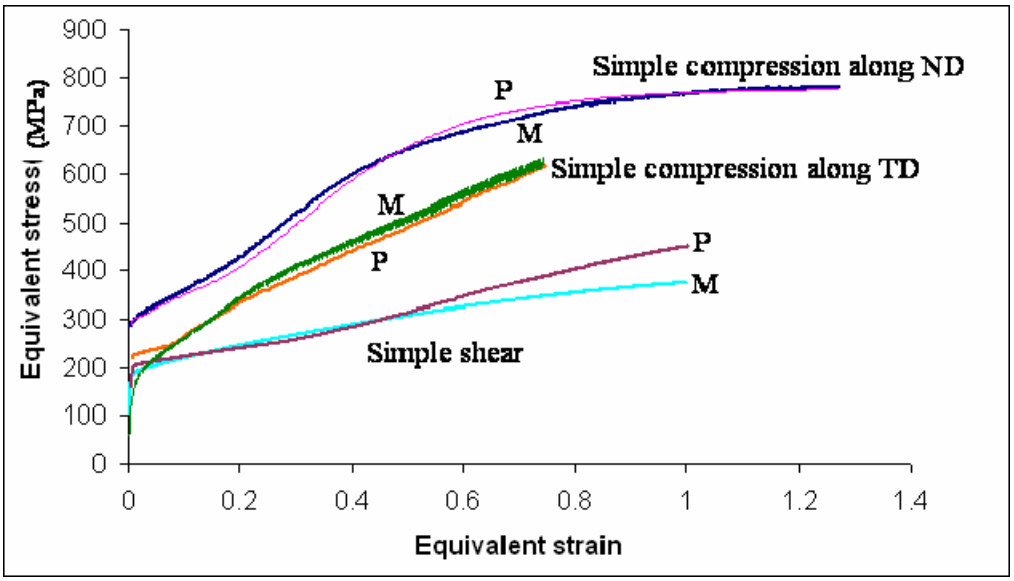

Figure 3. Comparison of predicted (P) and measured (M) equivalent stress-equivalent strain curves for different deformation modes on high purity α-Ti.

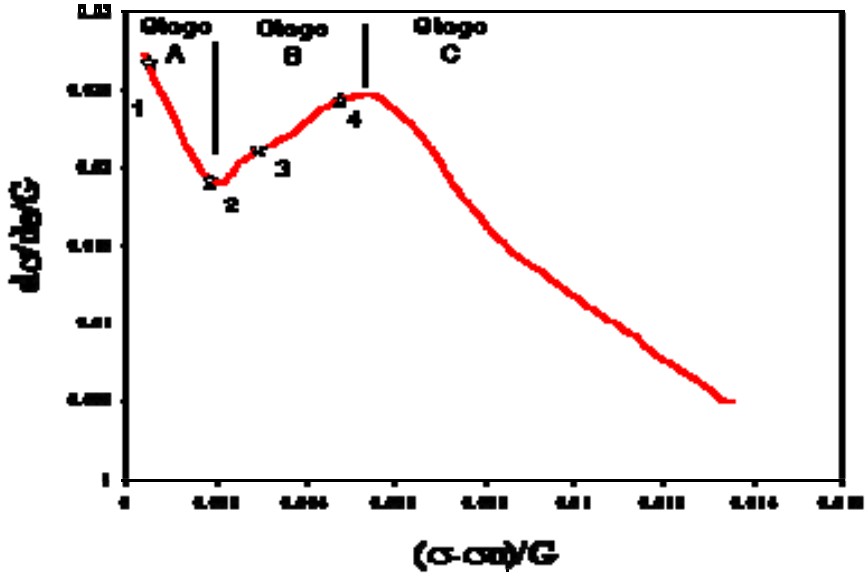

Figure 4. Strain hardening response of α-Ti in simple compression along ND. The ordinate is the normalized slope of the stress-strain curve and the abscissa is the normalized plastic flow stress, and G is theoretical shear modulus.

Using above strategy, the values of all model parameters were established (see Table2).

Table2. Summary of Parameter Values

Model parameters	s_o^{pri}	s_o^{bas}	s_o^{pyr}	s_{tw}	$h_{so}^{pri-bas}$	h_{so}^{pyr}
Values	30MPa	150MPa	120MPa	125MPa	15MPa	300MPa
Model parameters	s_{so}^{pri}	$s_{so}^{bas-pyr}$	s_{pr}	C	b	
Values	100MPa	300MPa	100MPa	25	2	

3.2 Evaluation: comparison with measurements

In this section, the proposed model and hardening laws were evaluated quantitatively by directly comparing the predictions to the measurements that were not used in the calibration process. The predicted stress-strain response in simple compression along TD showed excellent agreement with the measurement (see Figure 3). It is worth noting that the starting texture for the compression test along TD is significantly different compared to the starting texture for compression test along ND (see Figure 5). Note also that the flow stress in compression along TD is substantially lower than the flow stress in compression along ND (see Figure 3). The predicted stress-strain response for simple shear also showed good agreement with measurement up to strain $\gamma \approx 0.6$, but an overestimation of about 20% on flow stress is observed at large strain ($\gamma \approx 1.0$; see Figure 3). It is worth noting that at large shear strains the shear samples often develop macroscale shear bands and this could lower the measured flow stresses.

The stress-strain curves in Figure 3 were plotted as equivalent stress – equivalent strain curves. While the concept of a Mises-equivalent stress has no relevance for anisotropic plasticity, it helps us understand the degree of anisotropy exhibited by the material. If the material exhibited isotropic plastic response, all of the curves shown in Figure 3 should be identical. The spread between the stress-strain responses in the different modes (about a factor of 2 between simple compression and simple shear) in this figure provides us a measure of the degree of anisotropy

exhibited by the high purity α-Ti that is largely attributable to the underlying crystallographic texture in the sample. This degree of anisotropy appears to be well captured by the Taylor-type crystal plasticity model presented in this paper.

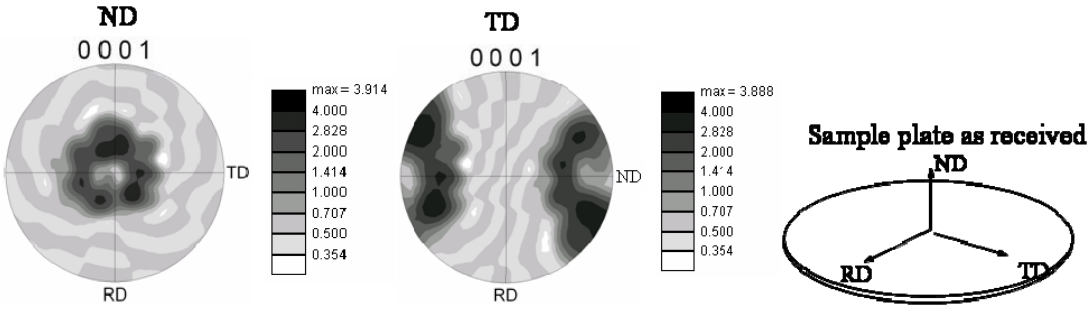

Figure 5. Comparison of initial texture for compression tests on α-Ti along ND and TD. The compressed samples were cut from a circular plate.

Texture predictions for simple compression along ND at two strains ($\varepsilon = -0.22$ and $\varepsilon = -1.00$) showed excellent agreement with the measurements (see Figure 6 and Figure 7). At $\varepsilon = -0.22$, both the prediction and the measurement exhibit two major c-axis fiber texture components (easily seen in (0001) pole figure). The first fiber has its c-axis about 15-30° from ND, while the second fiber has its c-axis about 75-90° from ND. The first component was associated with matrix, and the second component with twinning, in a prior study [19]. A similar texture is observed in (0001) pole figure at $\varepsilon = -1.00$, where the intensity of the component associated with twinning increased substantially.

Measurement

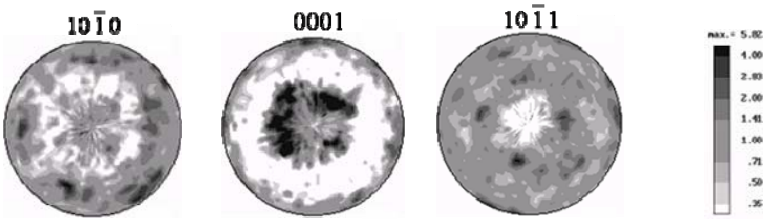

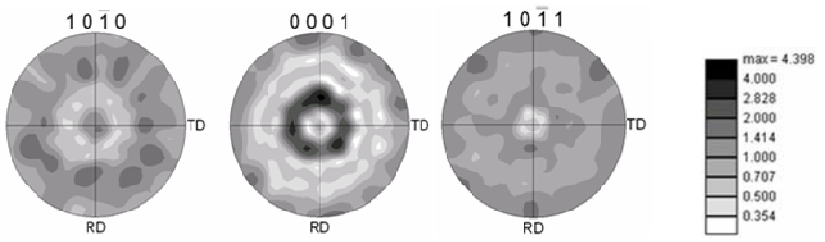

Prediction

Figure 6. Comparison of predicted and measured textures at $\varepsilon = -0.22$ in simple compression of α-Ti along ND.

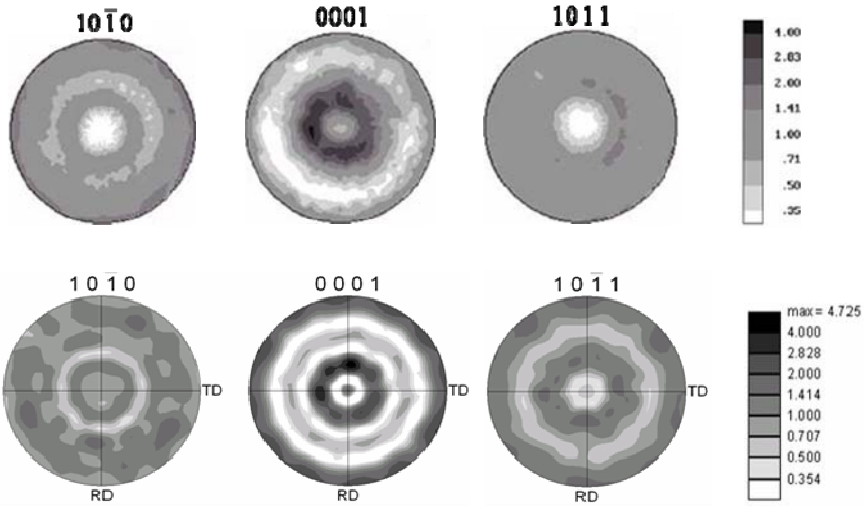

Measurement

Prediction

Figure 7. Comparison of predicted and measured textures at $\varepsilon = -1.00$ in simple compression of α–Ti along ND.

Texture predictions for simple shear at $\gamma = -1.00$ showed reasonable agreement with the corresponding measurement (see Figure 8), especially in the $(10\bar{1}0)$ pole figure where six strong texture components are clearly seen. The predicted (0001) pole figure captured the strong texture component located about 20-40° from ND. However, the predicted (0001) pole figures missed the weaker texture components located around the rim (see Figure 8).

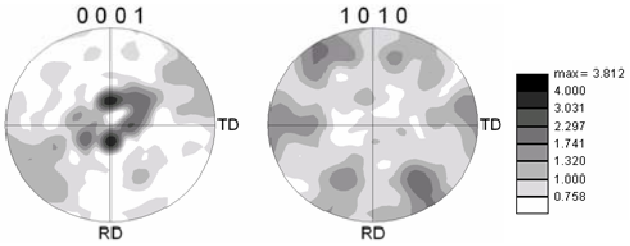

Measurement

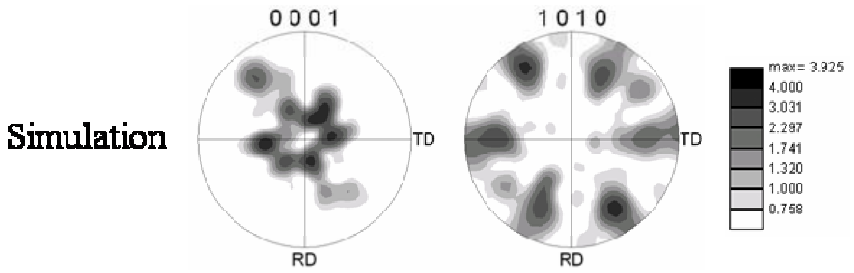

Figure 8. Comparison of predicted and measured textures at $\gamma = -1.00$ in simple shear of α-Ti.

3.3 Discussion

The polycrystal plasticity model presented here is built on the Taylor assumption of uniform deformation gradient in all of the constituent grains. It should be intuitively expected that this gross simplification should have a strong effect on the predictions. In fact, it should be expected that the effect of the Taylor assumption would be stronger on the hcp metals studied here compared to the more plastically isotropic cubic metals studied in previous work [1, 2, 8, 11, 27]. It is our intuition that many of the discrepancies reported here between the measurements and the predictions are all attributable to the Taylor assumption employed in this study. We are currently attempting to implement the crystal plasticity model described here in a finite element framework which averts the need for the simplifying Taylor assumption.

We also note that only monotonic deformation paths have been studied thus far. There is therefore a clear need to extend the studies described here to deformation path change experiments. It is anticipated that such studies will help us improve further the hardening descriptions [36-38].

4. Conclusions

A new crystal plasticity model has been formulated to simulate the anisotropic stress-strain response and texture evolution for α-titanium during large plastic strains at room temperature. The major new features of the model include: (a) incorporation of slip inside twins as an

significant contributor to accommodating the overall imposed plastic deformation, and (b) extension of slip and twin hardening laws to treat separately the hardening behavior of the different slip families (prismatic<a>, basal<a>, and pyramidal <c+a>) using hardening parameters that are all coupled to the extent of deformation twinning in the sample. Reasonable agreement between model predictions and the measurements has been observed for both the anisotropic stress-strain responses and the deformation texture evolution in three different monotonic deformation paths: (1) simple compression along ND, (2) simple compression along TD, (3) simple shear in the RD-TD plane.

Acknowledgements

The authors wish to acknowledge the many discussions with Prof. R. D. Doherty on various aspects of this study. This work was supported by a research grant from NSF (DMR-0201382). AAS was support through Air Force contract number F33615-03-D-5801.

References

1. Delannay, L., S.R. Kalidindi, and P. Van Houtte, *Quantitative prediction of textures in aluminium cold rolled to moderate strains.* Materials Science and Engineering A, 2002. **336**(1-2): p. 233-244.
2. Kalidindi, S.R., C.A. Bronkhorst, and L. Anand, *Crystallographic Texture Evolution in Bulk Deformation Processing of Fcc Metals.* Journal of the Mechanics and Physics of Solids, 1992. **40**(3): p. 537-569.
3. Asaro, R.J., *Crystal Plasticity.* Journal of Applied Mechanics, 1983. **50**(4b): p. 921-934.
4. Asaro, R.J. and A. Needleman, *Texture development and strain hardening in rate dependent polycrystals.* Acta Metallurgica et Materialia, 1985. **33**(6): p. 923-953.
5. Mathur, K. K., and P.R. Dawson, *On modelling the development of crystallographic texture in bulk forming processes.* International Journal of Plasticity, 1989. **5**: p. 67-94.
6. Kothari, M. and L. Anand, *Elasto-viscoplastic constitutive equations for policrystalline metals: application to tantalum.* J. Mech. Phys. Solids, 1998. **46**(1): p. 51-83.
7. Van Houtte, P., L. Delannay, and S.R. Kalidindi, *Comparison of two grain interaction models for polycrystal plasticity and deformation texture prediction.* International Journal of Plasticity, 2002. **18**(3): p. 359-377.
8. Bachu, V. and S.R. Kalidindi, *On the accuracy of the predictions of texture evolution by the finite element technique for FCC polycrystals.* Materials Science and Engineering A, 1998. **257**(1): p. 108-117.

9. Christian, J.W. and S. Mahajan, *Deformation twinning.* Progress in Materials Science, 1995. **39**(1-2): p. 1-157.
10. Singh, R.P. and R.D. Doherty, *Strengthening in MULTIPHASE (MP35N) alloy - Ambient temperature deformation and recrystallization.* Metallurgical Transactions A, 1992. **23**: p. 307-320.
11. El-Danaf, E., S.R. Kalidindi, and R.D. Doherty, *Influence of deformation path on the strain hardening behavior and microstructure evolution in low SFE FCC metals.* International Journal of Plasticity, 2001. **17**(9): p. 1245-1265.
12. Salem, A.A., S.R. Kalidindi, and R.D. Doherty, *Strain hardening of titanium: role of deformation twinning.* Acta Materialia, 2003. **51**(14): p. 4225-4237.
13. Santhanam, A.T. and R.E. Reed-Hill, *The influence of strain rate dependent work hardening on the necking strain in α-titanium at elevated temperatures.* Metall Trans, 1971. **2**(9): p. 2619.
14. Nourbakhsh, S. and T.D. O'Brien, *Texture formation and transition in cold-rolled titanium* Materials Science and Engineering, 1988. **100**(1-2): p. 109.
15. Gray III, G.T., *Influence of strain rate and temperature on the structure, property behavior of high-purity titanium.* Journal De Physique IV, 1997. **Colloque C3**: p. 423.
16. Nemat-Nasser, S., W.G. Guo, and J.Y. Cheng, *Mechanical properties and deformation mechanisms of a commercially pure titanium.* Acta Materialia, 1999. **47**(13): p. 3705-3720.
17. Salem, A.A., S.R. Kalidindi, and R.D. Doherty, *Strain hardening regimes and microstructure evolution during large strain compression of high purity titanium.* Scripta Materialia, 2002. **46**(6): p. 419-423.
18. Salem, A.A., S.R. Kalidindi, and R.D. Doherty, *Microstructure evolution and strain hardening mechanisms in titanium.* Acta Materialia, 2003.
19. Salem, A.A., et al., *Strain hardening due to deformation twinning in α-titanium: mechanisms* Metall Trans A, 2006. **37A**: p. 259.
20. Van Houtte, P., *Simulation of the rolling and shear texture of brass by the Taylor theory adapted for mechanical twinning.* Acta Metallurgica et Materialia, 1978. **26**(4): p. 591-604.
21. Tome, C.N., R.A. Lebensohn, and U.F. Kocks, *A model for texture development dominated by deformation twinning: Application to zirconium alloys.* Acta Metall, 1991. **39**(11): p. 2667-2680.
22. Staroselsky, A. and L. Anand, *Inelastic deformation of polycrystalline face centered cubic materials by slip and twinning.* Journal of the Mechanics and Physics of Solids, 1998. **46**(4): p. 671-696.
23. Staroselsky, A. and L. Anand, *A constitutive model for hcp materials deforming by slip and twinning: application to magnesium alloy AZ31B* International Journal of Plasticity 2003. **19**: p. 1843-1864.
24. Kaschner, G.C. and C.N. Tome, *Role of twinning in the hardening response of zirconium during temperature reloads* Acta Materialia, 2006. **02**: p. 36.
25. Bunge, H.-J., *Texture analysis in materials science. Mathematical Methods*. 1993, Göttingen: Cuvillier Verlag.
26. Kalidindi, S.R., *Incorporation of deformation twinning in crystal plasticity models.* Journal of the Mechanics and Physics of Solids, 1998. **46**(2): p. 267-271.

27. Kalidindi, S.R., *Modeling anisotropic strain hardening and deformation textures in low stacking fault energy fcc metals*, in *International Journal of Plasticity*. 2001. p. 837-860.
28. Kalidindi, S.R., A.A. Salem, and R.D. Doherty, *Role of deformation twinning on strain hardening in cubic and hexagonal polycrystalline metals.* Advanced Engineering Materials, 2003. **5**(4): p. 229-232.
29. Salem, A.A., S.R. Kalidindi, and S.L. Semiatin, *Strain hardening due to deformation twinning in α-titanium: Constitutive relations and crystal-plasticity modeling* Acta Materialia, 2005. **53**: p. 3495-3502.
30. Gurtin, M.E., *An introduction to continuum mechanics*. 1981, New York: Academic Press.
31. Asgari, S., et al., *Strain hardening regimes and microstructural evolution during large strain compression of low stacking fault energy fcc alloys that form deformation twins.* Metallurgical and Materials Transactions A: Physical Metallurgy and Materials Science, 1997. **28A**(9): p. 1781-1795.
32. Paton NE, W.J., *The deformation of α-phase titanium* Titanium Science and Technology 1973. **2**: p. 1049-1069.
33. Song, S.G. and I. Gray, G. T., *Structural interpretation of the nucleation and growth of deformation twins in Zr and Ti--II. Tem study of twin morphology and defect reactions during twinning.* Acta Metallurgica et Materialia, 1995. **43**(6): p. 2339-2350.
34. Taylor, G.I., *Plastic strain in metals.* Journal of the Institute of Metals, 1938. **62**: p. 307-324.
35. Kallend, J.S., et al., *Operational texture analysis.* Materials Science & Engineering A: Structural Materials: Properties, Microstructure and Processing, 1991. **A132**(1-2): p. 1-11.
36. Peeters, B., et al., *A theoretical investigation of the influence of dislocation sheets on evolution of yield surfaces in single-phase BCC polycrystals.* Journal of the Mechanics and Physics of Solids, 2002. **50**(4): p. 783-807.
37. Peeters, B., et al., *A crystal plasticity based work-hardening/softening model for b.c.c metals under changing strain paths.* Acta Materialia, 2000. **48**(9): p. 2123-2133.
38. Peeters, B., et al., *Work-hardening/softening behaviour of b.c.c. polycrystals during changing strain paths: I. An integrated model based on substructure and texture evolution, and its prediction of the stress-strain behaviour of an IF steel during two-stage strain paths.* Acta Materialia, 2001. **49**(9): p. 1607-1619.